

PYP1-4 peptide from *Pyropia yezoensis* protects against acetaminophen-induced hepatotoxicity in HepG2 cells

IN-HYE KIM^{1*}, JEONG-WOOK CHOI^{1*} and TAEK-JEONG NAM^{1,2}

¹Cell Biology Laboratory, Institute of Fisheries Sciences, Pukyong National University, Busan 46041;

²Department of Food Science and Nutrition, Pukyong National University, Busan 48513, Republic of Korea

Received December 14, 2018; Accepted October 15, 2019

DOI: 10.3892/etm.2019.8304

Abstract. Acetaminophen (APAP) is a widely used analgesic and antipyretic. It is safe at normal treatment doses; however, APAP overdose is a major cause of acute liver and kidney failure. A variety of methods to reduce the damage caused by APAP overdose have previously been evaluated. The protein-rich seaweed *Pyropia yezoensis* has antioxidant, anti-tumor and anti-inflammatory activities, and protects against cytotoxicity. However, little is known regarding the protective effects of *P. yezoensis* peptide against APAP-induced hepatotoxicity. The present study investigated the ability of *P. yezoensis* peptide (PYP1-4) to ameliorate the damage caused by APAP-induced hepatotoxicity using HepG2 as the model cell line in addition to the signaling pathways involved. Briefly, cell viability, nitric oxide, reactive oxygen species and apoptosis assays were performed in conjunction with western blot analysis and reverse transcription-quantitative PCR. First, the present study revealed the minimum toxic concentration of APAP (15 mM) and the resting concentration of PYP1-4 (0-500 ng/ml). Administration of PYP1-4 to APAP-induced cells decreased the nitric oxide and reactive oxygen species levels, and restored the levels of antioxidant-associated proteins (catalase, heme oxygenase 1, superoxide dismutase 2 and quinone oxidoreductase 1). PYP1-4 increased the translocation of nuclear factor, erythroid 2 like 2 to the nucleus and the activities of glycogen synthase kinase-3 β , Akt and AMP-activated protein kinase. In addition, APAP induced apoptosis; however, PYP1-4 inhibited apoptosis by modulating the levels of pro-apoptotic markers (Bad), anti-apoptotic markers (Bcl-2 and BH3 interacting domain death agonist), caspases and poly (ADP-ribose) polymerase 1. Subsequently, the insulin-like

growth factor 1 receptor signaling pathway was investigated to determine whether PYP1-4 treatment restored the levels of cell growth-associated factors during APAP-induced hepatotoxicity. PYP1-4 treatment impacted the levels of components of the insulin receptor substrate 1/PI3K/Akt and Ras/Raf/ERK signaling pathways, and promoted cell survival. Therefore, the *P. yezoensis* peptide PYP1-4 may be useful for preventing APAP-induced hepatotoxicity.

Introduction

Acetaminophen (APAP) is an effective analgesic and antipyretic (1,2). APAP is safe at therapeutic doses, and higher doses can be provided to patients for short durations (3). However, the incidence of APAP poisoning is increasing (4). In the United States and in the United Kingdom, APAP overdose has been reported as a major cause of drug-induced liver failure (5,6). Since APAP overdose causes severe damage to liver and kidney cells in humans and experimental animals (7,8), a number of studies have focused on the prevention or treatment of APAP-induced liver failure (9,10).

The mechanism of APAP-induced hepatotoxicity has been established and extensively reviewed (11,12). The liver failure that follows APAP ingestion is not due to the drug itself, but to a toxic metabolite, N-acetyl-p-benzoquinone imine, produced by the cytochrome P450 group of enzymes in the liver. This metabolite is normally rendered harmless through its interaction with glutathione (GSH), an endogenous antioxidant (11,12). However, when this APAP metabolite is overproduced, GSH stores in the liver become depleted, the metabolite accumulates, and tissue injury occurs (13). As a result, APAP overdose stimulates the apoptotic and/or necrotic death signaling pathways in cellular models (14,15). Additionally, APAP overdose increases oxidative stress and reactive oxygen species (ROS) levels, decreases GSH levels, induces mitogen-activated protein kinase (MAPK) signaling pathways, and activates caspase cascades (15-17). Furthermore, APAP overdose leads to liver failure, promoting lipid peroxidation and transcriptional activation of inflammatory factors (11,18). Based on this mechanism, several inhibitors of APAP overdose-induced liver and kidney failure, such as N-acetylcysteine (NAC) have been developed (19).

Seaweeds have received increased research attention, since the majority contain polysaccharides, proteins,

Correspondence to: Professor Taek-Jeong Nam, Department of Food Science and Nutrition, Pukyong National University, 45 Yongso-ro, Nam-gu, Busan 48513, Republic of Korea
E-mail: namtj@pknu.ac.kr

*Contributed equally

Key words: *Pyropia yezoensis*, peptide, acetaminophen, hepatotoxicity, insulin-like growth factor 1 receptor, apoptosis

vitamins and minerals with diverse biological activities (20). *Pyropia yezoensis*, a marine red alga, is cultured and consumed mainly in China, Japan and Korea (21). *P. yezoensis* produces free radicals and other potent oxidizing agents without causing serious photodynamic damage if exposed to adverse environmental conditions, such as a high light intensity or oxygen concentration (22,23). Therefore, *P. yezoensis* produces compounds that protect against external factors, including environmental pollutants, stresses and UV radiation (22,23). *P. yezoensis* has antioxidant (24,25), antitumor (26,27) and anti-inflammatory activities (28,29), and protects against neuronal senescence (30,31), photo-aging (22,23) and cytotoxicity (32,33).

A 14-kDa glycoprotein extracted from *P. yezoensis* reportedly protects against hepatotoxicity in rats with APAP-induced liver injury (33). After the protein is purified from the glycoprotein by protein sequencing and mass spectrometry, 10- and 7-kDa proteins are obtained (34). Treatment of the 10-kDa protein (protein ID PYP1; Rhod_EST AV429545) with digestive enzymes, including chymotrypsin, pepsin and trypsin, yields several peptides, which have been screened to identify those with protective effects (34).

Studies on the protective effects of *P. yezoensis* peptides in APAP-induced hepatotoxicity have produced inconclusive results (33,34). Therefore, the present study investigated the protective effects of *P. yezoensis* peptides on APAP-induced liver injury in HepG2 human liver cancer cells, as well as the underlying molecular mechanisms.

Materials and methods

Peptide synthesis. The peptide PYP1-4 (A-T-R-D-P-E-P-T-A-V-D-P-N) from *P. yezoensis* was commercially synthesized by Pepton Corporation and purified to >95% purity. PYP1-4 was purified using a Shimadzu Prominence high-performance liquid chromatography system with a C18 column (Capcell Pak; Shiseido Co., Ltd.), using the Class-VP software (version 6.14; Shimadzu Corporation). PYP1-4 was first dissolved in 0.1% trifluoroacetic acid/water at 1 mg/ml and 40 μ l of the solution was then injected into the HPLC system. The HPLC system condition was as follows: Acetonitrile gradient, 10-40%; flow rate, 1 ml/min, temperature, 50°C; and UV detection, 220 nm. The molecular weight of PYP1-4 was 1,382 Da as determined by mass spectrometry (HP 1100 Series LC/MSD; Agilent Technologies, Inc.) using ionization mode (positive + H, 1.0079 Da; negative - H, -1.0079 Da) and multiple reaction monitoring (300-2,300 m/z). The synthesized peptides was reconstituted in water (10 mg/ml) and stored at -50°C.

Cell culture. HepG2 liver cancer cells (cat. no. HB-8065) were purchased from the American Type Culture Collection. The cells were cultured at 37°C with 5% CO₂ in minimum essential medium (MEM; Sigma-Aldrich; Merck KGaA) supplemented with 10% FBS (GenDEPOT) containing 50 μ g/ml penicillin, 25 μ g/ml amphotericin B and 50 μ g/ml streptomycin. The medium was replaced every 2 days.

Cell viability assay. Cell viability was estimated using a Cyto X Cell Viability Assay kit (cat. no. CYT3000; LPS solution). Cells were seeded in 96-well plates at 2x10⁴ cells/well in 100 μ l

medium and allowed to attach for 24 h at 37°C. Attached cells were then treated with PYP1-4 (125, 250 or 500 ng/ml) and 15 mM APAP (A7085; Sigma-Aldrich; Merck KGaA) in serum-free MEM (SFM) for 18 h at 37°C. Cyto X solution was added to the cells, followed by incubation for 1 h at 37°C and the absorbance at a wavelength of 450 nm was measured using a FilterMAX F5 microplate reader (Molecular Devices LLC). Morphological changes to the cells were subsequently observed using a light microscope (magnification, x200; Eclipse TS100-F; Nikon Corporation).

Nitric oxide (NO) assay. The nitrite concentration in culture medium was determined spectrophotometrically as described previously by Lee *et al.* (29). Briefly, cells were seeded in 48-well plates at 2x10⁶ cells/well and incubated for 24 h at 37°C. The cells were treated with PYP1-4 (125, 250 or 500 ng/ml) and 15 mM APAP in SFM for 18 h at 37°C. Subsequently, 100 μ l culture medium were transferred to a 96-well plate, and 100 μ l Griess reagent (G4410; Sigma-Aldrich; Merck KGaA) was added. The plate was incubated for 10 min at 37°C, following which absorbance at a wavelength of 540 nm was measured using a FilterMAX F5 microplate reader.

Intracellular ROS assay. The intracellular ROS concentration was assayed using the ROS-sensitive fluorescent dye 2',7'-dichlorofluorescein diacetate (DCF-DA; cat. no. 35845; Sigma-Aldrich; Merck KGaA). Cells were seeded in 96-well plates at 2x10⁵ cells/well and incubated for 24 h at 37°C. The cells were treated with PYP1-4 (125, 250 or 500 ng/ml) and 15 mM APAP in SFM for 18 h at 37°C. Subsequently, the cells were incubated with 10 μ M DCF-DA at 37°C for 30 min. The fluorescence intensities of stained cells were measured using a FilterMAX F5 microplate reader at excitation and emission wavelengths of 485 and 535 nm, respectively.

Apoptosis assay. Apoptosis was assayed using the Muse[®] Annexin V and Dead Cell Assay Kit (cat. no. MCH100105; BD Biosciences). The cells were harvested and washed twice with PBS, and stained with FITC Annexin V and propidium iodide for 15 min at room temperature. The percentage of apoptotic cells was determined using Annexin V and dead cell software program of Muse[™] Cell Analyzer system (2013; EMD Millipore).

Western blot analysis. HepG2 cells were cultured for 18 h at 37°C in SFM containing 0, 125, 250 or 500 ng/ml PYP1-4 and 15 mM APAP. The cells were washed with PBS and lysed in RIPA lysis buffer (50 mM Tris-HCl, 1 mM EDTA, 150 mM sodium chloride, 1% NP-40 and 0.25% sodium deoxycholate; pH 7.4) containing protease inhibitors (1 μ g/ml aprotinin, 1 μ g/ml leupeptin, 1 μ g/ml pepstatin, 1 mM sodium orthovanadate, 1 mM sodium fluoride and 1 mM phenylmethanesulfonyl fluoride) on ice for 30 min. The extracts were centrifuged at 12,000 x g for 10 min at 4°C, and the supernatants were used for western blot analysis. Protein concentration was measured using the Bicinchoninic Acid protein assay kit. Total protein (30 μ g) was electrophoresed using a 10-15% acrylamide gel and transferred to PVDF transfer membranes (EMD Millipore). The membranes were blocked with 1% bovine serum albumin (BSA; GenDEPOT) in TBST (5 mM

Tris and 20 mM sodium chloride; pH 7.4; 0.1% Tween-20) and incubated with primary antibodies (dilution, 1:1,000) in 1% BSA-TBST with gentle agitation at 4°C overnight. The membranes were washed twice for 15 min each in TBST, incubated with the corresponding horseradish peroxidase (HRP)-conjugated secondary antibody (dilution, 1:10,000) for 2 h at room temperature, and then washed. Immunoreactive bands were detected using an enhanced chemiluminescence substrate (Advansta Inc.) and visualized using the GeneSys imaging system (SynGene; Synoptics Ltd.). Differences in protein levels were determined by semi-quantifying western blot band densities using ImageJ software (version IJ.146r; National Institutes of Health). The primary antibodies used in the present study are as follows: Anti-catalase (CAT; cat. no. OAAB05216; rabbit), anti-superoxide dismutase 1 (cat. no. OASE00355; rabbit), anti-superoxide dismutase 2 (SOD2; cat. no. OASE00357; rabbit; Aviva Systems Biology Corporation), anti-heme oxygenase 1 (HO1; cat. no. sc-1796; goat), anti-quinone oxidoreductase 1 (NQO1; cat. no. sc-16464; goat), anti-nuclear factor, erythroid 2 like 2 (Nrf2; cat. no. sc-722; rabbit), anti-phosphorylated-(p-)JNK (cat. no. sc-6254; mouse), anti-JNK (cat. no. sc-7345; mouse), anti-p- p38 MAP kinase (p38; cat. no. sc-7973; mouse), anti-p38 (cat. no. sc-7149; rabbit), anti-p-glycogen synthase kinase 3 β (GSK3 β ; cat. no. sc-81496; mouse), anti-GSK3 β (cat. no. sc-7291; mouse), anti-p-AMP-activated protein kinase (AMPK; cat. no. sc-33524; rabbit), anti-AMPK (cat. no. sc-74461; mouse), anti-Bcl-2 (cat. no. sc-492; rabbit), anti-Bcl-xL (cat. no. sc-7195; rabbit), anti-BH3 interacting domain death agonist (Bid; cat. no. sc-11423; rabbit), anti-poly (ADP-ribose) polymerase 1 (PARP; cat. no. sc-7150; rabbit), anti-caspase-9 (cat. no. sc-7885; rabbit), anti-caspase-3 (cat. no. sc-7148; rabbit), anti-Bad (cat. no. sc-7869; rabbit), anti-Bax (cat. no. sc-493; rabbit), anti-insulin-like growth factor 1 receptor (IGF-IR; cat. no. sc-390130; mouse), anti-epidermal growth factor receptor (EGFR; cat. no. sc-03; goat), anti-erb-b2 receptor tyrosine kinase 2 (ErbB2; cat. no. sc-284; rabbit), anti-erb-b2 receptor tyrosine kinase 3 (ErbB3; cat. no. sc-285; rabbit), anti-insulin receptor substrate 1 (IRS-1; cat. no. sc-560; rabbit), anti-PI3K (cat. no. sc-374534; mouse), anti-PTEN (cat. no. sc-7974; mouse), anti-pyruvate dehydrogenase kinase 1 (cat. no. sc-28783; rabbit), anti-p-Akt (cat. no. sc-7985; rabbit), anti-Akt (cat. no. sc-8312; rabbit), anti-p-mTOR (cat. no. sc-293132; mouse), anti-mTOR (cat. no. sc-8319; rabbit), anti-p70S6 kinase (p70S6K; cat. no. sc-8418; mouse), anti-eukaryotic translation initiation factor 4E (eIF4E; cat. no. sc-514875; mouse), anti-SHC adaptor protein 1 (SHC; cat. no. sc-967; mouse), anti-growth factor receptor bound protein 2 (GRB2; cat. no. sc-255; rabbit), anti-SOS Ras/Rac guanine nucleotide exchange factor 1 (SOS; cat. no. sc-259; rabbit), anti-Ras (cat. no. sc-520; rabbit), anti-Raf (cat. no. sc-227; rabbit), anti-p-mitogen-activated protein kinase kinase (MEK; cat. no. sc-81503; mouse), anti-MEK (cat. no. sc-81504; mouse), anti-p-ERK (cat. no. sc-7383; mouse), anti-ERK (sc-292838; rabbit, Santa Cruz Biotechnology, Inc.). The anti- β -actin (cat. no. sc-47778; mouse) antibody was used as a control. The secondary antibodies were HRP-conjugated anti-mouse IgG (cat. no. 32430), anti-rabbit IgG (cat. no. 31460) and anti-goat IgG (cat. no. 31400; Invitrogen; Thermo Fisher Scientific, Inc.).

Reverse transcription-semi-quantitative PCR. Total RNA was extracted from HepG2 cells using a QIAzol Lysis Reagent kit (Qiagen Sciences, Inc.). Reverse transcription was performed using AccuPower RT PreMix (Bioneer Corporation) according to the manufacturer's protocol. PCR amplification was performed using the template cDNA (1 ng). The reverse transcribed cDNA was amplified using a PCR premix kit (dNTP mix, *nTaq* Buffer and *nTaq*; Enzynomics), and the following specific primer pairs (Cosmogenetech Co., Ltd.) were used: IGF-IR forward, 5'-ACAACCTACGCCCTGGTCATC-3' and reverse, 5'-TGGCAGCACTCATTTGTTCTC-3'; EGFR forward, 5'-TGGATTTCATCAGCATTTGGA-3' and reverse, 5'-GCACCTGTAAAATGCCCTGT-3'; ErbB2 forward, 5'-CTACGGCAGAGAACCAGAG-3' and reverse, 5'-ACA CCATTGCTGTTCCCTTCC-3'; ErbB3 forward, 5'-GCGGCA CTTTTCTCTACTGG-3' and reverse, 5'-GGTCAGCCACAC CAAAATCT-3'; and β -actin forward, 5'-AAATCTGGCACC ACACCTTC-3' and reverse, 5'-AGCACTGTGTTGGCGTAC AG-3'. Reaction mixtures were subjected to initial denaturation at 95°C for 3 min, followed by 34 cycles of 95°C for 30 sec, 55-60°C for 30 sec and 72°C for 60 sec, then a final extension of 72°C for 5 min. The products were normalized to β -actin as an internal control and separated by electrophoresis using a 1% agarose gel and stained with 0.5 μ g/ml ethidium bromide for detection. Signal intensities were examined using a bio-imaging system (MiniBis Pro; DNR Bio-Imaging Systems, Ltd.). The software GeneTools version 4.03 (Syngene Europe) was used for densitometric analysis.

Statistical analysis. Results are presented as the mean \pm SD of three independent experiments. The significance of differences among multiple means was assessed by one-way or two-way ANOVA followed by Bonferroni's multiple comparison test using GraphPad Prism software (version 7; GraphPad Software, Inc.). $P < 0.05$ was considered to indicate a statistically significant difference.

Results

PYP1-4 protects against APAP-induced toxicity in HepG2 cells. The present study assessed the effect of 0-500 ng/ml PYP1-4 on HepG2 cell viability. Treatment with PYP1-4 alone appeared to have significantly increased cell viability, but no significance differences between concentrations were observed (Fig. 1A). Subsequently, a survival rate of 60% was selected following treatment with 15 mM APAP for 18 h. The cell viability of the APAP overdose group was 61.5 \pm 2.4% compared with the control (Fig. 1B). Treatment with 15 mM APAP and 125, 250 and 500 ng/ml PYP1-4 significantly restored cell viability to 64.9 \pm 1.8, 69.9 \pm 3.0 and 75.9 \pm 1.4%, respectively, compared with the control. Microscopic observations confirmed these results (Fig. 1C).

PYP1-4 decreases APAP-induced oxidative stress in HepG2 cells. Oxidative stress is involved in APAP-induced liver failure, and liver tissue is damaged by various cytokines and high levels of NO following an APAP overdose (35). Griess reagent was used to investigate NO production in HepG2 cells treated with PYP1-4 and APAP overdose. The APAP overdose group exhibited a significantly higher NO level (130.5 \pm 9.9%) than the

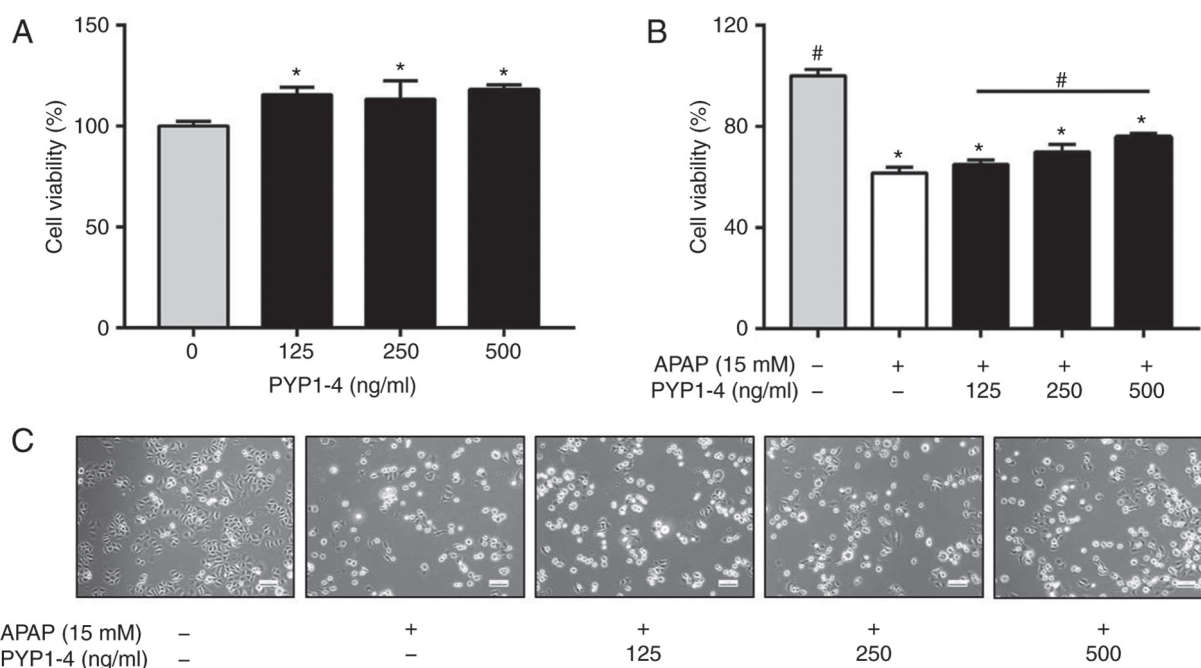


Figure 1. PYP1-4 promotes the survival of APAP-induced HepG2 cells. HepG2 cells were incubated with (A) the indicated concentrations of PYP1-4 for 18 h or (B) PYP1-4 (125-500 ng/ml) in the presence or absence of 15 mM APAP for 18 h. Cell viability was assessed using a Cyto X assay, and the results are presented as percentages of surviving cells compared with the control (non-treated group). (C) Cell morphological alterations were observed under a light microscope. Magnification, $\times 200$. Data are presented as the mean \pm SD of three independent experiments and were analyzed using two-way ANOVA. * $P < 0.05$ vs. control group; # $P < 0.05$ vs. the 15 mM APAP group. APAP, acetaminophen; PYP1-4, *P. yezoensis* peptide.

control group, whereas co-treatment with PYP1-4 significantly suppressed the NO level in a concentration-dependent manner (Fig. 2A). In the 500 ng/ml PYP1-4 group, NO production was reduced to $100.2 \pm 11.8\%$ compared with the APAP overdose group ($130.5 \pm 9.9\%$).

APAP-induced toxicity increases ROS levels and promotes oxidative stress (36-38). The present study investigated ROS levels in HepG2 cells using the fluorescent dye DCF-DA following treatment with PYP1-4 and APAP overdose. The ROS level was significantly higher in the APAP overdose group ($184.6 \pm 16.6\%$) than in the control group (Fig. 2B). However, PYP1-4 co-treatment reduced the ROS level compared with that in the APAP overdose group, in a concentration-dependent manner (165.9 ± 16.1 , 129.1 ± 19.8 and $107.9 \pm 10.1\%$ for 125, 250 and 500 ng/ml PYP1-4, respectively).

Subsequently, the levels of antioxidant enzymes, including CAT, HO1, SOD and NQO1 were investigated by western blotting. The APAP overdose group exhibited lower protein levels of CAT, HO1 and SOD2 than the control group, whereas PYP1-4 co-treatment significantly increased the CAT, HO1, SOD2 and NQO1 levels in a concentration-dependent manner (Fig. 2C and D).

To investigate the role of PYP1-4 in the modulation of MAPK signaling in APAP-induced cells, the phosphorylation levels of JNK and p38 were determined by western blotting. The phosphorylation levels were 2.7-fold (JNK) and 2.0-fold (p38) higher in the APAP overdose group than in the control group, whereas co-treatment with PYP1-4 significantly inhibited the phosphorylation of JNK and p38 compared APAP overdose group (Fig. 2C and D). p-JNK/JNK phosphorylation was significantly decreased in the PYP1-4 co-treatment groups compared with in the APAP group in

a concentration-dependent manner (2.8-, 2.3- and 1.3-fold, respectively). Similarly, p-p38/p38 was significantly decreased (1.9-, 1.6- and 1.2-fold, respectively).

PYP1-4 increases Nrf2 expression and phosphorylation of GSK3 β , Akt and AMPK in APAP-induced HepG2 cells. AMPK increases the inhibitory phosphorylation of GSK3 β upstream of Akt (39) and phosphorylation of GSK3 β stimulates Nrf2 (40,41). To identify the upstream effector of activation of Nrf2 by PYP1-4, the role of AMPK in PYP1-4-induced Akt/GSK3 β phosphorylation and Nrf2 nuclear translocation was investigated in the present study. The APAP overdose group exhibited reduced HO1 and Nrf2 levels, as well as reduced ratios of p-GSK3 β /GSK3 β and p-AMPK/AMPK, compared with the control group (Fig. 3). However, PYP1-4 co-treatment groups significantly induced the expression and nuclear translocation of Nrf2, as well as the phosphorylation of GSK3 β , Akt and AMPK in HepG2 cells.

PYP1-4 inhibits APAP-induced apoptosis. Toxic APAP doses reportedly induce apoptosis of murine hepatocytes (42,43). Therefore, the induction of apoptosis by APAP was investigated using FITC Annexin V assays in the present study. The apoptosis ratio was significantly higher in the APAP overdose group (43.2%) compared with the control group (4.77%; Fig. 4A). However, the cell survival rate was increased and the apoptosis ratio was significantly decreased in the PYP1-4 co-treatment groups compared with in the APAP group in a concentration-dependent manner (34.2, 26.6 and 20.2%, respectively).

To investigate the molecular mechanism by which PYP1-4 suppresses apoptosis, the present study examined its effect on the expression levels of Bcl-2-family proteins, which

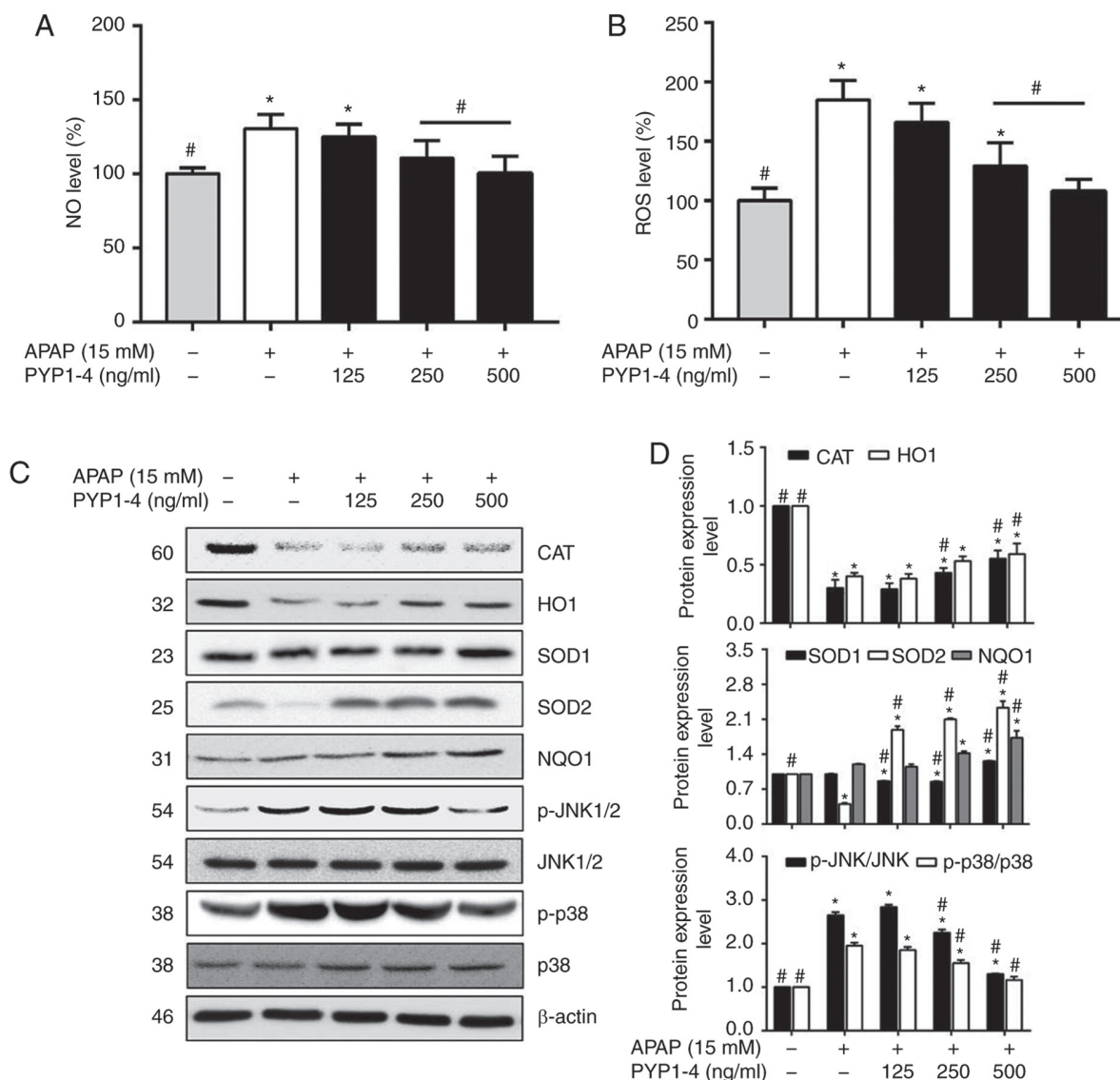


Figure 2. PYP1-4 treatment restores APAP-induced oxidative stress in APAP-induced HepG2 cells. (A) HepG2 cells were incubated with 15 mM APAP with or without various concentrations of PYP1-4 for 18 h. NO levels were analyzed using a Griess assay. (B) ROS levels were analyzed by 2',7'-dichlorofluorescein diacetate assay. (C) Levels of oxidative stress-associated proteins (CAT, HO1, SOD1, SOD2, NQO1, JNK and p38) were determined by western blot analysis. (D) Bands were normalized to β -actin as an internal control, and the phosphorylated vs. total protein ratio was graphed. Data are presented as the mean \pm SD of three independent experiments and were subjected to two-way ANOVA. * $P < 0.05$ vs. the control group; # $P < 0.05$ vs. the 15 mM APAP group. APAP, acetaminophen; NO, nitric oxide; PYP1-4, *P. yezoensis* peptide; ROS, reactive oxygen species; CAT, catalase; HO1, heme oxygenase 1; SOD1, superoxide dismutase 1; SOD2, superoxide dismutase 2; NQO1, quinone oxidoreductase 1; p-, phosphorylated; p38, p38 MAP kinase.

regulate apoptosis by controlling mitochondrial membrane permeability and cytochrome *c* release (44), in APAP-induced HepG2 cells. The levels of pro-apoptotic (Bad and Bax) and anti-apoptotic (Bcl-2, Bcl-xL and Bid) Bcl-2-family proteins were examined. The PYP1-4 co-treatment groups exhibited lower Bad levels and higher Bcl-2 and Bid levels than the APAP overdose group, in a concentration-dependent manner (Fig. 4B and C).

Additionally, the present study demonstrated that PYP1-4 activated caspases. The PYP1-4 co-treatment groups exhibited increased expression levels of caspase-9 and caspase-3 compared with the APAP group in a concentration-dependent manner. Additionally, PARP cleavage in the PYP1-4 co-treatment groups was significantly decreased compared with that in the APAP group, in a concentration-dependent manner (Fig. 4B and C).

PYP1-4 reverses the effects of overdose on the levels of growth-associated receptors. PYP1-4 co-treatment reversed the effects of APAP overdose on apoptosis and survival. The present study assessed the protein and RNA levels of IGF-IR, EGFR, ErbB2 and ErbB3, based on the assumption that the increased cell survival was associated with effects on growth-associated receptors. PYP1-4 co-treatment groups increased the protein levels of IGF-IR and EGFR compared with APAP overdose (Fig. 5). However, the RNA levels of these receptors were unaffected, with the exception of ErbB3.

PYP1-4 increases the levels of IRS-1/PI3K/Akt signaling pathway-associated proteins in APAP-induced cells. IGF signaling affects cell survival, and the IGF-I protein level is elevated in HepG2 cells (45). PYP1-4 co-treatment restored APAP-induced apoptosis and the levels of growth factor

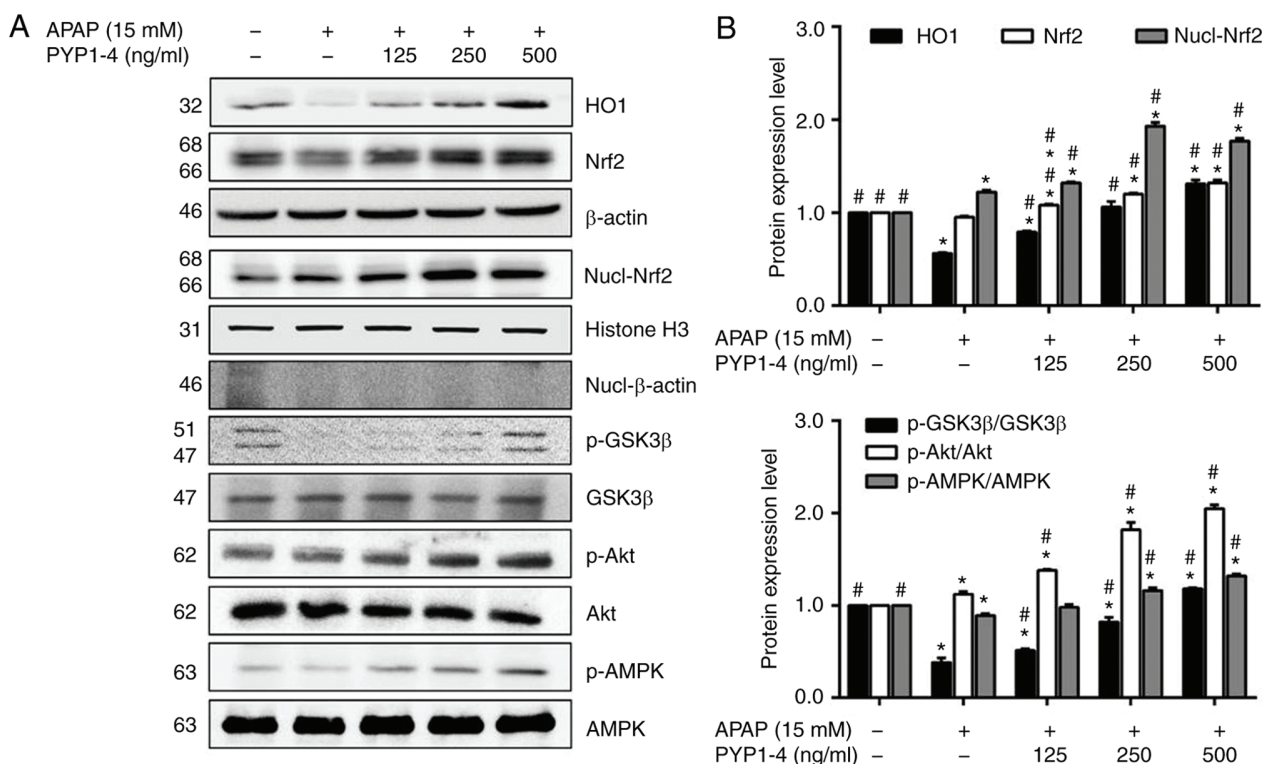


Figure 3. Effect of PYP1-4 on AMPK activation is required for Akt/GSK3 β -mediated Nrf2 activity. (A) HepG2 cells were incubated with 15 mM APAP with or without various concentrations of PYP1-4 for 18 h. Levels of Nrf2-associated proteins (HO1, Nrf2, GSK3 β , Akt and AMPK) were determined by western blot analysis. (B) Bands were normalized to β -actin and histone H3 as internal controls, and the phosphorylated vs. total protein ratio was graphed. Data are presented as the mean \pm SD of three independent experiments and were subjected to two-way ANOVA. * P <0.05 vs. control group; # P <0.05 vs. 15 mM APAP group. AMPK, protein kinase AMP-activated catalytic subunit α 2; APAP, acetaminophen; GSK3 β , glycogen synthase kinase 3 β ; HO1, heme oxygenase 1; Nrf2, nuclear factor, erythroid 2 like 2; p-, phosphorylated-; PYP1-4, *P. yezoensis* peptide.

receptors (Figs. 4 and 5). Subsequently, the levels of proteins associated with the IRS-1/PI3K/Akt signaling pathway, one of the two major downstream IGF-IR signaling pathways (46), were assessed. PYP1-4 co-treatment groups significantly increased the protein levels of IGF-IR, IRS-1, PI3Kp85, PTEN, p70S6K and eIF4E in a concentration-dependent manner compared with the levels in the APAP overdose group (Fig. 6). In addition, PYP1-4 co-treatment groups significantly increased ratios of p-Akt/Akt and p-mTOR/mTOR compared with the ratios in the APAP overdose group.

PYP1-4 increases the levels of Ras/Raf/ERK signaling pathway-associated proteins in APAP-induced cells. Subsequently, the present study investigated the levels of proteins associated with the Ras/Raf/ERK signaling pathway, which is the other major IGF-IR downstream signaling pathway (47). PYP1-4 co-treatment groups significantly increased the protein levels of IGF-IR, SHC, SOS and GRB2 in a concentration-dependent manner compared with the APAP group (Fig. 7). In addition, PYP1-4 co-treatment groups significantly increased the levels of p-MEK/MEK and p-ERK/ERK compared with those in the APAP group.

Discussion

Seaweeds have attracted attention from researchers due to their abundance of polysaccharides, proteins, vitamins, minerals and polyphenols (48,49). Seaweeds, including brown, green

and red algae, possess anti-obesogenic, anticancer, antioxidant and anti-inflammatory activities due to various bioactive compounds (50). The red alga *P. yezoensis* is of increasing interest due to its rich sugars and protein content (51). Although numerous studies on have been investigated the polysaccharide and polyphenol constituents of *P. yezoensis* (22-24,26,28,31,32,52), studies on the proteins contained in this alga remain lacking (25,27,29,30,33,34).

APAP is safe at therapeutic doses; however, excessive doses cause serious hepatotoxicity in laboratory animals and humans, and are a major cause of liver and kidney failure (3,7,8). Therefore, methods to reduce the hepatotoxicity of APAP overdose are required.

Studies on seaweeds and APAP-induced hepatotoxicity have focused on *Sargassum* species (*Hizikia fusiformis*, syn. *Sargassum fusiforme*), red algae (*P. yezoensis*), green algae (*Ulva reticulata* and *Chlorella sorokiniana*) and sulfated polysaccharides (fucoidan) (33,53-56). In a previous study, prevention of APAP-induced hepatotoxicity is associated with a 14-kDa protein (PYP) of *P. yezoensis* (33). PYP may inhibit APAP-induced GSH depletion in rats. APAP also increases caspase-3 activity during apoptosis, DNA fragmentation and serum glutamic oxaloacetic transaminase/glutamic pyruvic transaminase levels, which are indicators of hepatic damage (33). Additionally, co-treatment with PYP and APAP reversed these effects to the levels in the control (33). Therefore, although further studies are required, there is evidence to support that PYP inhibits APAP-induced hepatotoxicity.

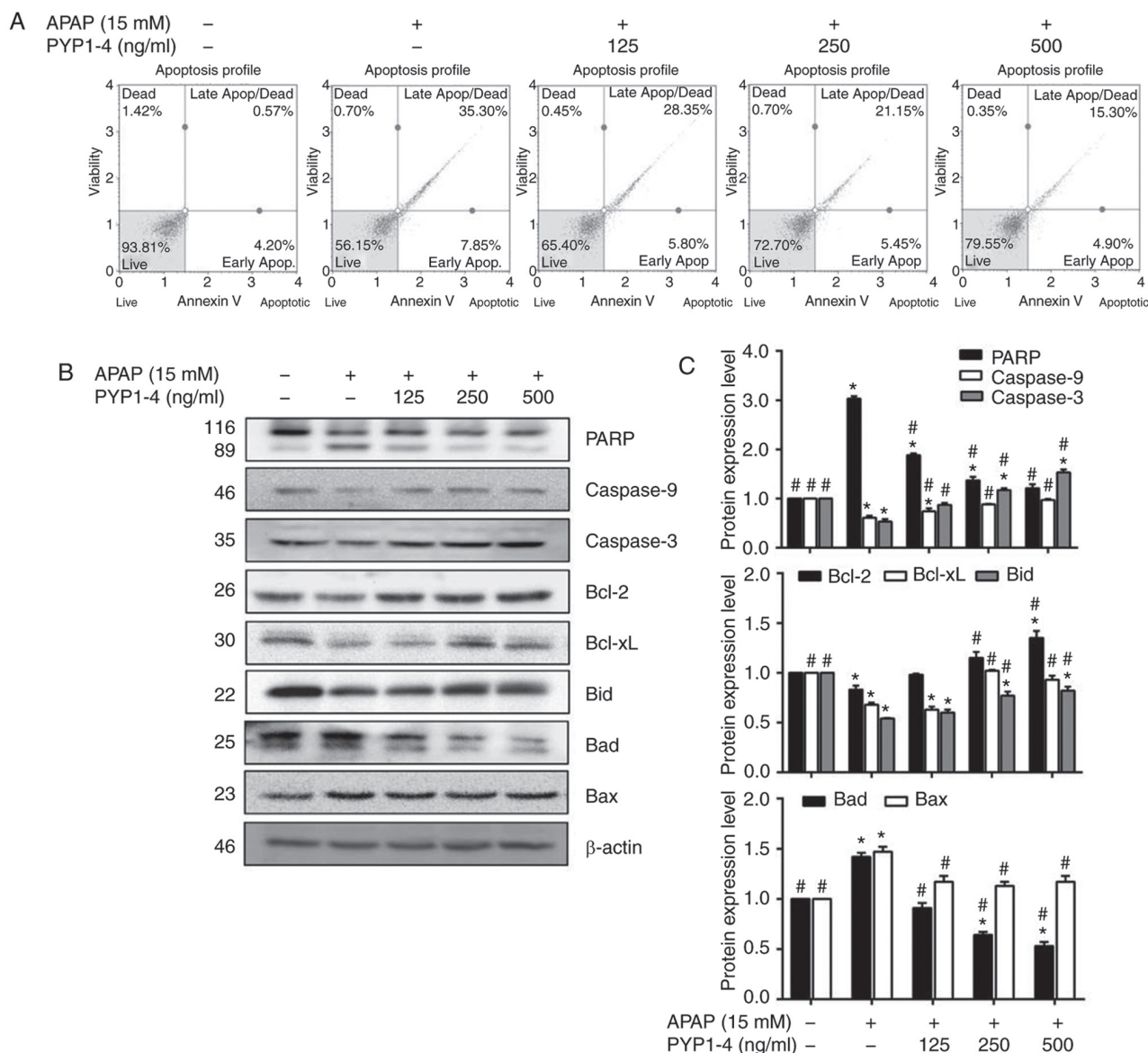


Figure 4. PYP1-4 treatment suppresses APAP-induced apoptosis of HepG2 cells. (A) HepG2 cells were incubated with 15 mM APAP with or without various concentrations of PYP1-4 for 18 h. FITC Annexin V flow cytometry was employed to determine the percentages of apoptotic and necrotic cells. (B) Levels of apoptosis-associated proteins (PARP, caspase-9, caspase-3, Bcl-2, Bcl-xL, Bid, Bad and Bax) were determined by western blot analysis. (C) Bands were normalized to β -actin as an internal control, and protein levels were graphed. Data are presented as the mean \pm SD of three independent experiments, and were subjected to two-way ANOVA. * $P < 0.05$ vs. control group; # $P < 0.05$ vs. 15 mM APAP group. APAP, acetaminophen; Apop, apoptosis; Bid, BH3 interacting domain death agonist; PARP, poly(ADP-ribose) polymerase 1; PYP1-4, *P. yezoensis* peptide.

Based on these results, PYP has been purified from the 14-kDa protein using SDS-PAGE, automated protein sequencing and matrix assisted laser desorption/ionization quadrupole ion trap-time-of-flight mass spectrometry (34). The PYP fraction contains two proteins, PYP1 (10 kDa; an SDS-resistant dimer) and PYP2 (10 kDa) (34). Based on these results, the synthetic peptide PYP1 (1-20) corresponding to the N-terminal 20 residues of PYP1 (ALEGGKSSGGGEATRDPEPT) has been obtained (34). PYP1 (1-20) protects against APAP-induced apoptosis in HeLa (Chang Liver) cells, and has been determined to be the active fraction of PYP (34).

The present study investigated the protective effects of *P. yezoensis* peptides on APAP-induced hepatotoxicity. In a previous study, a total of 13 peptides were obtained by treating PYP1 (1-20) with trypsin, chymotrypsin and pepsin (34). These

peptides were finally selected for PYP1-4 based on the cell viability assay results. The present study revealed that PYP1-4 at 0-500 ng/ml was non-toxic in HepG2 cells and reversed the effects of APAP-induced hepatotoxicity.

Activation of the Nrf2 signaling pathway serves an essential role in APAP-induced acute liver failure (57). Nrf2 is a redox-sensitive transcription factor and regulates the transcription of genes associated with protection against oxidative stress (58). In the cytoplasm, Nrf2 is typically present in the Nrf2-Kelch-like ECH-associated protein 1 (Keap1) complex (59). In response to oxidative stress, Nrf2 dissociates from Keap1 and translocates to the nucleus to induce the expression of genes encoding antioxidant enzymes (NQO1, glutathione S-transferase and HO1) by binding to the antioxidant response element in their promoters (60). Intracellular ROS

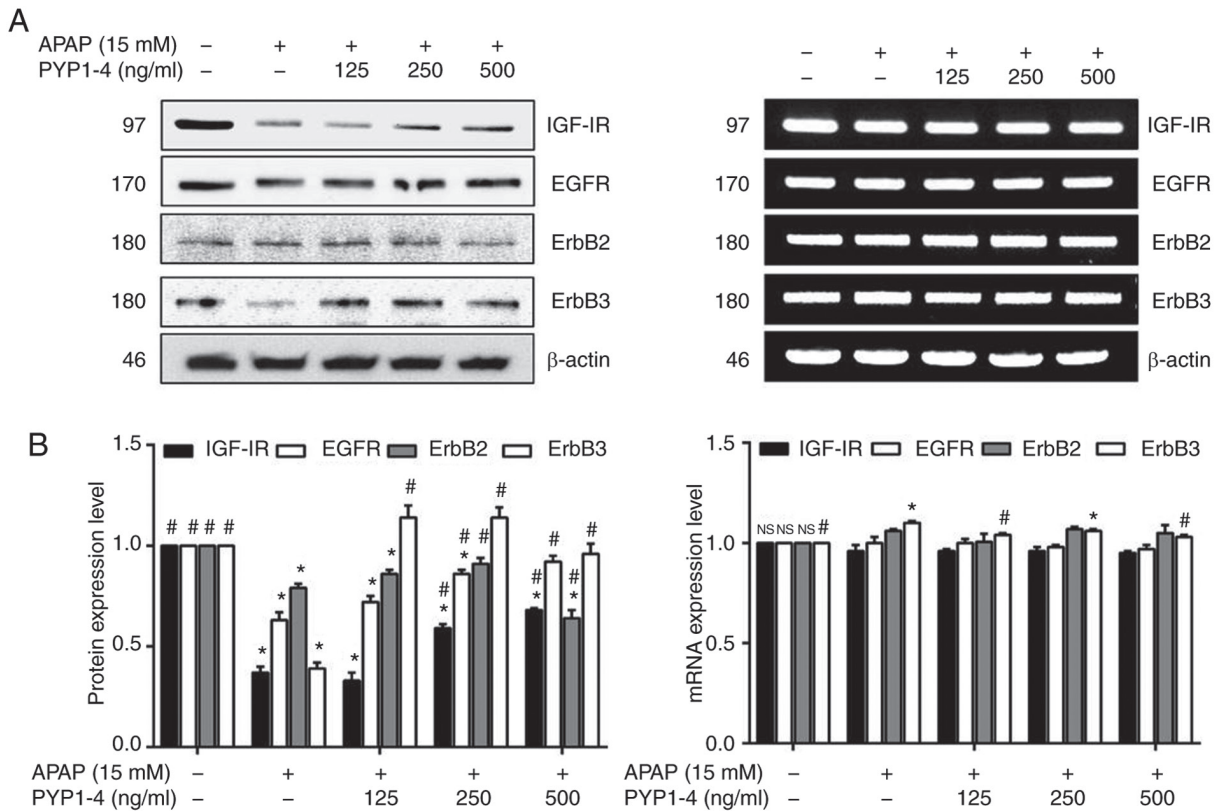


Figure 5. PYP1-4 treatment restores the levels of growth-associated factors in APAP-induced HepG2 cells. (A) HepG2 cells were incubated with 15 mM APAP with or without various concentrations of PYP1-4 for 18 h. The protein and RNA levels of growth-associated factors (IGF-IR, EGFR, ErbB2, and ErbB3) were determined by western blot analysis and reverse transcription PCR. (B) Bands were normalized to β-actin as an internal control, and protein and RNA levels were graphed. Data are presented as the mean ± SD of three independent experiments, and were subjected to two-way ANOVA. *P<0.05 vs. the control group; #P<0.05 vs. the 15 mM APAP group. APAP, acetaminophen; EGFR, epidermal growth factor receptor; ErbB2, erb-b2 receptor tyrosine kinase 2; ErbB3, erb-b2 receptor tyrosine kinase 3; IGF-IR, insulin-like growth factor 1 receptor; PYP1-4, *P. yezoensis* peptide.

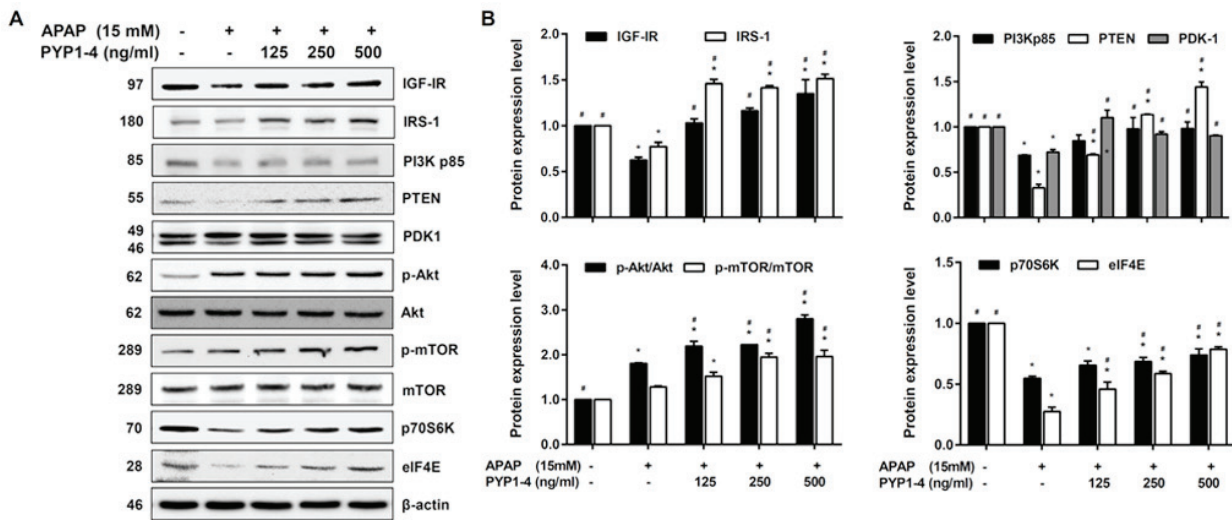


Figure 6. PYP1-4 restores the levels of IRS-1/PI3K/Akt signaling pathway proteins in APAP-induced HepG2 cells. (A) HepG2 cells were incubated with 15 mM APAP with or without various concentrations of PYP1-4 for 18 h. The levels of IRS-1/PI3K/Akt signaling pathway proteins (IGF-IR, IRS-1, PI3K, PTEN, PDK1, Akt, mTOR, p70S6K and eIF4E) were determined by western blot analysis. (B) Bands were normalized to β-actin as an internal control, and the phosphorylated vs. total protein ratios were graphed. Data are the means ± SD of three independent experiments and were subjected to two-way analysis of variance. *P<0.05 vs. control group; #P<0.05 vs. 15 mM APAP group. APAP, acetaminophen; eIF4E, eukaryotic translation initiation factor 4E; IGF-IR, insulin-like growth factor 1 receptor; IRS-1, insulin receptor substrate 1; p-, phosphorylated-; p70S6K, p70S6 kinase; PDK1, pyruvate dehydrogenase kinase 1; PYP1-4, *P. yezoensis* peptide.

accumulation disrupts the Nrf2-Keap1 interaction; oxidized Keap1 binds to the adapter protein GAP-associated tyrosine

phosphoprotein p62 and releases Nrf2, which translocates to the nucleus and activates transcription of genes encoding

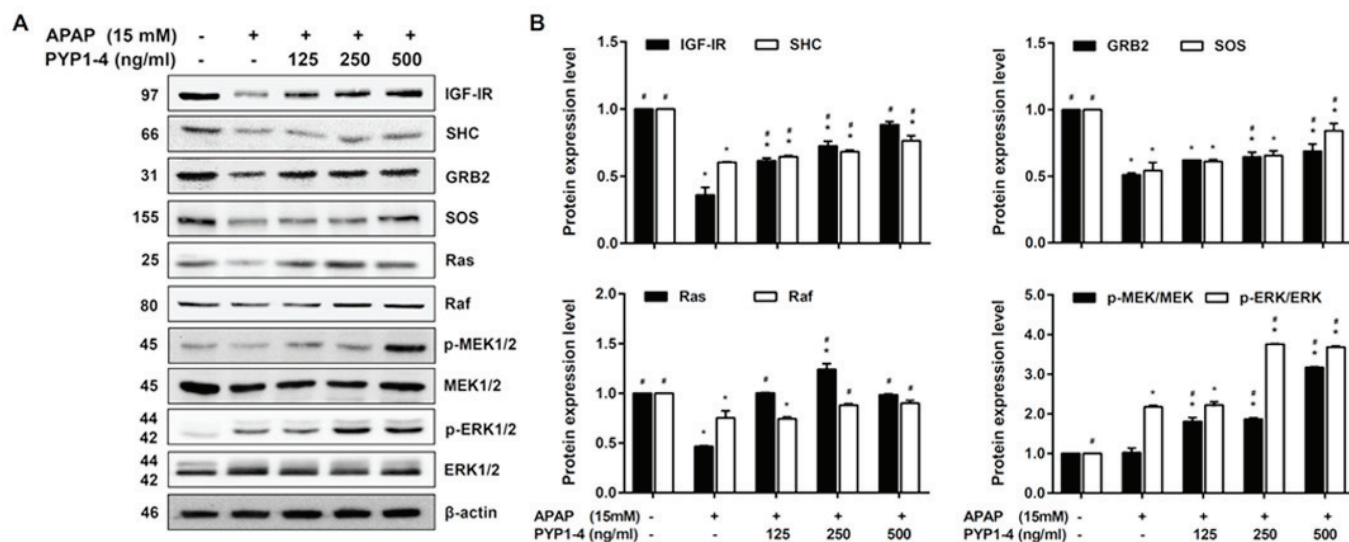


Figure 7. PYP1-4 restores the levels of Ras/Raf/ERK signaling pathway proteins in APAP-induced HepG2 cells. (A) HepG2 cells were incubated with 15 mM APAP with or without various concentrations of PYP1-4 for 18 h. The levels of Ras/Raf/ERK signaling pathway proteins (IGF-IR, SHC, GRB2, SOS, Ras, Raf, MEK and ERK) were determined by western blot analysis. (B) Bands were normalized to β -actin as an internal control, and the phosphorylated vs. total protein ratios were graphed. Data are presented as the mean \pm SD of three independent experiments, and were subjected to two-way ANOVA. * P <0.05 vs. control group; # P <0.05 vs. 15 mM APAP group. APAP, acetaminophen; GRB2, growth factor receptor bound protein 2; IGF-IR, insulin-like growth factor 1 receptor; MEK, mitogen-activated protein kinase kinase; p-, phosphorylated; PYP1-4, *P. yezoensis* peptide; SHC, SHC adaptor protein 1; SOS, SOS Ras/Rac guanine nucleotide exchange factor 1.

antioxidant and detoxifying enzymes (61). Therefore, Nrf2 has potential as a therapeutic target for liver diseases, including APAP-induced hepatotoxicity (62). In present study, the antioxidant activity of PYP1-4 contributes to its protective effect against APAP-induced hepatotoxicity, and this protective effect is associated with the activation of the Nrf2/HO1/SOD2 signaling pathway.

Additionally, Nrf2 can be activated by post-transcriptional modification by kinases, including protein kinase C, PI3K and MAPK (63,64). AMPK activates the PI3K/Akt signaling pathway, and Akt activation is essential for the phosphorylation of GSK3 β and may modulate oxidative stress (65). A heterotrimeric serine/threonine kinase, AMPK, senses the cellular energy status and regulates cell survival and death under oxidative stress (66). GSK3 β is a constitutively activated Ser/Thr protein kinase that regulates glycogen metabolism, gene expression and cell death (67). Previously, based on evidence that GSK3 β is a novel regulator of Nrf2, Nrf2 has been suggested to function in combination with the AMPK/Akt/GSK3 β signaling network (40,41). Therefore, regulation of the Nrf2 signaling pathway by PYP1-4 may ameliorate APAP-induced acute liver failure by modulating the AMPK/Akt/GSK3 β signaling pathway. In the present study, PYP1-4 increased Akt activity by phosphorylating GSK3 β , and PYP1-4-induced Akt activation stimulated Nrf2 activity. In addition, the increased GSK3 β phosphorylation caused by activation of AMPK protected against oxidative stress.

JNK phosphorylation and mitochondrial translocation increase mitochondrial dysfunction, and AMPK activation serves a crucial role in protecting mitochondria (68). In the present study, treatment with PYP1-4 activated AMPK, and inhibited the APAP-induced phosphorylation of JNK. These results suggested that PYP1-4 treatment protected against APAP-induced hepatotoxicity by inhibiting JNK

phosphorylation. Resveratrol has been reported to protect mitochondria against oxidative stress by increasing phosphorylation of GSK3 β by activating AMPK (68). In addition, esculetin A regulates Nrf2 activation via the AMPK/Akt/GSK3 β signaling pathway (69). These results suggest that PYP1-4 treatment exhibits an antioxidant effect by activating Nrf2 via the AMPK/Akt/GSK3 β pathway, thus protecting against APAP-induced hepatotoxicity (Fig. 3).

APAP-induced cell death remains controversial. The signal transduction pathways involved in apoptosis and necrosis exhibit a degree of overlap (70). In a previous study using ICR mice, 95% of APAP-damaged hepatocytes died due to necrosis *in vivo* (71); however, another study reported that APAP-induced hepatocyte (HuH7 cells) apoptosis serves a crucial role in liver failure (72). APAP-induced cell death has been hypothesized to be caused by necroptosis, which is characterized by features of necrosis and apoptosis (73). In the present study, APAP overdose increased apoptosis, whereas co-treatment with PYP1-4 resulted in a dose-dependent decrease in apoptosis.

Apoptosis can be initiated by intrinsic and/or extrinsic signaling pathways (73). Apoptosis of mammalian cells is regulated by Bcl-2 family proteins (44), which modulate mitochondrial membrane permeability and cytochrome *c* release. APAP induces metastasis of Bcl-2 family proteins (70), leading to the release of cytochrome *c*. Activation of apoptosis via the exogenous signaling pathway is mediated by the binding of an apoptotic ligand to a death receptor (74). These death receptors have intracellular domains that function as protein binding modules. Following recruitment and signaling of adapter molecules, cleavage and activation of pro-caspase-8, -9, -10 and -12 occur (75). This leads to the activation of caspase-3, -6 and -7, as well as the effector caspase, resulting in DNA fragmentation (75). In addition, APAP-induced hepatotoxicity occurs

via matrix metalloproteinase degradation of cytochrome *c* and activation of caspase-8, -9 and -3 (76). Cleaved PARP is a marker of apoptosis; PARP is activated in cells undergoing stress and/or DNA damage, and is inactivated by cleavage of caspase-3 during programmed cell death (76). Therefore, the results of the present study suggested that PYP1-4 inhibits APAP-induced apoptosis via intrinsic (endogenous) and extrinsic (exogenous) signaling pathways (Fig. 4).

Several studies have investigated the mechanism by which IGF-IR protects against apoptosis (45,77,78). During apoptosis, the binding of wild-type IGF-IR suppresses cell death. A previous study has demonstrated that APAP-induced HeLa (Chang Liver) cells were restored to apoptosis following treatment with IGF-I (79). The present study demonstrated that the IGF-IR signaling pathway was affected by PYP1-4.

IGFs are synthesized in and secreted by adult and fetal hepatocytes, widely expressed in a number of cell types, essential for normal growth, development and differentiation, and mediate signals for apoptosis inhibition, mitogenesis and immobilization-independent growth (45,80).

IGF-IR-associated signaling pathways comprise the IRS-1/PI3K/Akt and Ras/Raf/ERK signaling pathways (46,47). IGF-IR is autophosphorylated by intrinsic tyrosine kinase activity and promotes activation of downstream signaling molecules. The binding of activated IGF-IR and phosphorylated adaptor proteins such as IRS-1 then activate the PI3K/Akt signaling pathway (81,82). IRS-1/PI3K/Akt along with mTOR/p70S6K signaling activates translation initiation factors and inactivates regulatory factors (83). This signaling pathway is also involved in the crosstalk with the Ras/Raf/ERK signaling pathways (84). In addition, Ras signaling is enhanced by upstream events such as the activation of IGF-IR (85). Ras continuously stimulates the MAPK-activating serine/threonine kinase Raf and induces cell growth through transcriptional activation of multiple targets (86).

MAPKs, including ERK, JNK and p38, are part of the IGF-IR signaling pathway and convert extracellular stimuli into a wide range of cellular responses. These proteins serve important roles in cell proliferation, differentiation, metabolism, survival and death (87,88), as well as in oxidative damage (77,78). JNK is primarily involved apoptosis and is activated by oxidative damage, whereas ERK regulates cell growth and differentiation, is activated by oxidative damage, and acts as a cell death suppression signal to maintain homeostasis (89). Akt is a downstream target of the PI3K/Akt signaling pathway and serves an important role in the inhibition of PI3K-mediated cell proliferation (90). In the present study, PYP1-4 treatment of APAP-induced HepG2 cells induced growth and reduced oxidative damage and apoptosis in a dose-dependent manner on the IRS-1/PI3K/Akt and Ras/Raf/ERK signaling pathways.

In conclusion, the present study revealed that PYP1-4 decreased APAP-induced oxidative damage, growth inhibition and apoptosis in HepG2 cells. Additionally, the IGF-IR signaling pathway contributed to the suppression of apoptosis and necrosis. These observations suggested that PYP1-4 exerts a hepatoprotective effect against APAP-induced oxidative damage and apoptosis. However, further research on the structure of PYP1-4 and on the signal transduction pathways involved in APAP-induced hepatotoxicity is required.

Acknowledgements

Not applicable.

Funding

The present study was supported by the Basic Science Research Program through the National Research Foundation of Korea funded by the Ministry of Education (grant no. 2012R1A6A1028677).

Availability of data and materials

The datasets used and/or analyzed during the current study are available from the corresponding author on reasonable request.

Authors' contributions

IHK and TJN designed the experiments. IHK and JWC performed the experiments, interpreted the experimental results and drafted the manuscript. TJN and JWC performed revising the manuscript critically for important intellectual content. All authors read and approved the final manuscript.

Ethics approval and consent to participate

Not applicable.

Patient consent for publication

Not applicable.

Competing interests

The authors declare that they have no competing interests.

References

- Cuzzolin L, Antonucci R and Fanos V: Paracetamol (acetaminophen) efficacy and safety in the newborn. *Curr Drug Metab* 14: 178-185, 2013.
- Klotz U: Paracetamol (acetaminophen) - a popular and widely used nonopioid analgesic. *Arzneimittelforschung* 62: 355-359, 2012.
- Mazaleuskaya LL, Sangkuhl K, Thorn CF, FitzGerald GA, Altman RB and Klein TE: PharmGKB summary: Pathways of acetaminophen metabolism at the therapeutic versus toxic doses. *Pharmacogenet Genomics* 25: 416-426, 2015.
- Prescott LF: Hepatotoxicity of mild analgesics. *Br J Clin Pharmacol* 2 (Suppl 10): 373S-379S, 1980.
- Litovitz TL, Klein-Schwartz W, Rodgers GC Jr, Cobaugh DJ, Youniss J, Omslaer JC, May ME, Woolf AD and Benson BE: 2001 annual report of the american association of poison control centers toxic exposure surveillance system. *Am J Emerg Med* 20: 391-452, 2002.
- Blieden M, Paramore LC, Shah D and Ben-Joseph R: A perspective on the epidemiology of acetaminophen exposure and toxicity in the United States. *Expert Rev Clin Pharmacol* 7: 341-348, 2014.
- Simkin S, Hawton K, Kapur N and Gunnell D: What can be done to reduce mortality from paracetamol overdoses? A patient interview study. *QJM* 105: 41-51, 2012.
- Craig DG, Ford AC, Hayes PC and Simpson KJ: Systematic review: Prognostic tests of paracetamol-induced acute liver failure. *Aliment Pharmacol Ther* 31: 1064-1076, 2010.

9. Lee WM: Acetaminophen and the U.S. Acute Liver Failure Study Group: Lowering the risks of hepatic failure. *Hepatology* 40: 6-9, 2004.
10. Knight TR, Fariss MW, Farhood A and Jaeschke H: Role of lipid peroxidation as a mechanism of liver injury after acetaminophen overdose in mice. *Toxicol Sci* 76: 229-236, 2003.
11. Hinson JA, Roberts DW and James LP: Mechanisms of acetaminophen-induced liver necrosis. *Handb Exp Pharmacol* 196: 369-405, 2010.
12. Yoon E, Babar A, Choudhary M, Kutner M and Prysopoulos N: Acetaminophen-induced hepatotoxicity: A comprehensive update. *J Clin Transl Hepatol* 4: 131-142, 2016.
13. James LP, Mayeux PR and Hinson JA: Acetaminophen-induced hepatotoxicity. *Drug Metab Dispos* 31: 1499-1506, 2003.
14. Zhao X, Cong X, Zheng L, Xu L, Yin L and Peng J: Dioscin, a natural steroid saponin, shows remarkable protective effect against acetaminophen-induced liver damage in vitro and in vivo. *Toxicol Lett* 214: 69-80, 2012.
15. Liang YL, Zhang ZH, Liu XJ, Liu XQ, Tao L, Zhang YF, Wang H, Zhang C, Chen X and Xu DX: Melatonin protects against apoptosis-inducing factor (AIF)-dependent cell death during acetaminophen-induced acute liver failure. *PLoS One* 7: e51911, 2012.
16. Slitt AM, Dominick PK, Roberts JC and Cohen SD: Effect of ribose cysteine pretreatment on hepatic and renal acetaminophen metabolite formation and glutathione depletion. *Basic Clin Pharmacol Toxicol* 96: 487-494, 2005.
17. Yousef MI, Omar SA, El-Guendi MI and Abdelmegid LA: Potential protective effects of quercetin and curcumin on paracetamol-induced histological changes, oxidative stress, impaired liver and kidney functions and haematotoxicity in rat. *Food Chem Toxicol* 48: 3246-3261, 2010.
18. Yan M, Huo Y, Yin S and Hu H: Mechanisms of acetaminophen-induced liver injury and its implications for therapeutic interventions. *Redox Biol* 17: 274-283, 2018.
19. Corcoran GB, Todd EL, Raczy WJ, Hughes H, Smith CV and Mitchell JR: Effects of N-acetylcysteine on the disposition and metabolism of acetaminophen in mice. *J Pharmacol Exp Ther* 232: 857-863, 1985.
20. Shahidi F and Rahman J: Bioactive in seaweeds, algae, and fungi and their role in health promotion. *J Food Bioact* 2: 58-81, 2018.
21. Niwa K: Genetic analysis of artificial green and red mutants of *Porphyra yezoensis* Ueda (Bangiales, Rhodophyta). *Aquaculture* 308: 6-12, 2010.
22. Kim S, You DH, Han T and Choi EM: Modulation of viability and apoptosis of UVB-exposed human keratinocyte HaCaT cells by aqueous methanol extract of laver (*Porphyra yezoensis*). *J Photochem Photobiol B* 141: 301-307, 2014.
23. Ryu J, Park SJ, Kim IH, Choi YH and Nam TJ: Protective effect of porphyra-334 on UVA-induced photoaging in human skin fibroblasts. *Int J Mol Med* 34: 796-803, 2014.
24. Ma XT, Sun XY, Yu K, Gui BS, Gui Q and Ouyang JM: Effect of content of sulfate groups in seaweed polysaccharides on antioxidant activity and repair effect of subcellular organelles in injured HK-2 cells. *Oxid Med Cell Longev* 2017: 2542950, 2017.
25. Toyosaki T and Iwabuchi M: New antioxidant protein in seaweed (*Porphyra yezoensis* Ueda). *Int J Food Sci Nutr* 60 (Suppl 2): 46-56, 2009.
26. Yu X, Zhou C, Yang H, Huang X, Ma H, Qin X and Hu J: Effect of ultrasonic treatment on the degradation and inhibition cancer cell lines of polysaccharides from *Porphyra yezoensis*. *Carbohydr Polym* 117: 650-656, 2015.
27. Park SJ, Ryu J, Kim IH, Choi YH and Nam TJ: Activation of the mTOR signaling pathway in breast cancer MCF-7 cells by a peptide derived from *Porphyra yezoensis*. *Oncol Rep* 33: 19-24, 2015.
28. Yanagido A, Ueno M, Jiang Z, Cho K, Yamaguchi K, Kim D and Oda T: Increase in anti-inflammatory activities of radical-degraded porphyrans isolated from discolored nori (*Pyropia yezoensis*). *Int J Biol Macromol* 117: 78-86, 2018.
29. Lee HA, Kim IH and Nam TJ: Bioactive peptide from *Pyropia yezoensis* and its anti-inflammatory activities. *Int J Mol Med* 36: 1701-1706, 2015.
30. Oh JH, Kim EY and Nam TJ: Phycoerythrin-derived tryptic peptide of a red alga *Pyropia yezoensis* attenuates glutamate-induced ER stress and neuronal senescence in primary rat hippocampal neurons. *Mol Nutr Food Res* 62: e1700469, 2018.
31. Mohibullah M, Bhuiyan MM, Hannan MA, Getachew P, Hong YK, Choi JS, Choi IS and Moon IS: The edible red alga *Porphyra yezoensis* promotes neuronal survival and cytoarchitecture in primary hippocampal neurons. *Cell Mol Neurobiol* 36: 669-682, 2016.
32. Choi JW, Kim IH, Kim YM, Lee MK and Nam TJ: *Pyropia yezoensis* glycoprotein regulates antioxidant status and prevents hepatotoxicity in a rat model of D-galactosamine/lipopolysaccharide-induced acute liver failure. *Mol Med Rep* 13: 3110-3114, 2016.
33. Hwang HJ, Kwon MJ, Kim IH and Nam TJ: Chemoprotective effects of a protein from the red algae *Porphyra yezoensis* on acetaminophen-induced liver injury in rats. *Phytother Res* 22: 1149-1153, 2008.
34. Choi YH, Yamaguchi K, Oda T and Nam TJ: Chemical and mass spectrometry characterization of the red alga *Pyropia yezoensis* chemoprotective protein (PYP): Protective activity of the N-terminal fragment of PYP1 against acetaminophen-induced cell death in chag liver cells. *Int J Mol Med* 35: 271-276, 2015.
35. Wallace JL: Acetaminophen hepatotoxicity: NO to the rescue. *Br J Pharmacol* 143: 1-2, 2004.
36. Liu WX, Jia FL, He YY and Zhang BX: Protective effects of 5-methoxypsoralen against acetaminophen-induced hepatotoxicity in mice. *World J Gastroenterol* 18: 2197-2202, 2012.
37. Olaleye MT and Rocha BT: Acetaminophen-induced liver damage in mice: Effects of some medicinal plants on the oxidative defense system. *Exp Toxicol Pathol* 59: 319-327, 2008.
38. Lee KJ, You HJ, Park SJ, Kim YS, Chung YC, Jeong TC and Jeong HG: Hepatoprotective effects of *Platycodon grandiflorum* on acetaminophen-induced liver damage in mice. *Cancer Lett* 174: 73-81, 2001.
39. Zheng T, Yang X, Wu D, Xing S, Bian F, Li W, Chi J, Bai X, Wu G, Chen X, *et al*: Salidroside ameliorates insulin resistance through activation of a mitochondria-associated AMPK/PI3K/Akt/GSK3 β pathway. *Br J Pharmacol* 172: 3284-3301, 2015.
40. Mathur A, Rizvi F and Kakkar P: PHLPP2 down regulation influences nuclear Nrf2 stability via Akt-1/Gsk3 β /Fyn kinase axis in acetaminophen induced oxidative renal toxicity: Protection accorded by morin. *Food Chem Toxicol* 89: 19-31, 2016.
41. Xing HY, Cai YQ, Wang XF, Wang LL, Li P, Wang GY and Chen JH: The cytoprotective effect of hyperoside against oxidative stress is mediated by the Nrf2-ARE signaling pathway through GSK-3 β inactivation. *PLoS One* 10: e0145183, 2015.
42. Song E, Fu J, Xia X, Su C and Song Y: Bazhen decoction protects against acetaminophen induced acute liver injury by inhibiting oxidative stress, inflammation and apoptosis in mice. *PLoS One* 9: e107405, 2014.
43. Sharma S, Singh RL and Kakkar P: Modulation of Bax/Bcl-2 and caspases by probiotics during acetaminophen induced apoptosis in primary hepatocytes. *Food Chem Toxicol* 49: 770-779, 2011.
44. Cory S, Huang DC and Adams JM: The Bcl-2 family: Roles in cell survival and oncogenesis. *Oncogene* 22: 8590-8607, 2003.
45. Yao NH, Yao DF, Dong ZZ, Yan XD, Chen J, Yao M, Wang L and Yan MJ: Effects of inhibited IGF-IR expression on proliferation and apoptosis of human hepatocellular carcinoma cell lines. *Zhonghua Gan Zang Bing Za Zhi* 21: 376-380, 2013 (In Chinese).
46. Kulik G, Klippel A and Weber MJ: Antiapoptotic signalling by the insulin-like growth factor I receptor, phosphatidylinositol 3-kinase, and Akt. *Mol Cell Biol* 17: 1595-1606, 1997.
47. Yu H and Rohan T: Role of the insulin-like growth factor family in cancer development and progression. *J Natl Cancer Inst* 92: 1472-1489, 2000.
48. MacArtain P, Gill CI, Brooks M, Campbell R and Rowland IR: Nutritional value of edible seaweeds. *Nutr Rev* 65: 535-543, 2007.
49. Dawczynski CH, Schubert R and Jahreis G: Amino acids, fatty acids, and dietary fiber in edible seaweed products. *Food Chemistry* 103: 891-899, 2007.
50. Lee JC, Hou MF, Huang HW, Chang FR, Yeh CC, Tang JY and Chang HW: Marine algal natural products with anti-oxidative, anti-inflammatory, and anti-cancer properties. *Cancer Cell Int* 13: 55, 2013.
51. Qu W, Ma H, Pan Z, Luo L, Wang Z and He R: Preparation and antihypertensive activity of peptides from *Porphyra yezoensis*. *Food Chem* 123: 14-20, 2010.
52. Ueno M, Cho K, Isaka S, Nishiguchi T, Yamaguchi K, Kim D and Oda T: Inhibitory effect of sulphated polysaccharide porphyrin (isolated from *Porphyra yezoensis*) on RANKL-induced differentiation of RAW264.7 cells into osteoclasts. *Phytother Res* 32: 452-458, 2018.

53. Hira K, Sultana V, Ara J and Haque SE: Protective role of Sargassum species in liver and kidney dysfunctions and associated disorders in rats intoxicated with carbon tetrachloride and acetaminophen. *Pak J Pharm Sci* 30: 721-728, 2017.
54. Balaji Raghavendra Rao H, Sathivel A and Devaki T: Antihepatotoxic nature of *Ulva reticulata* (Chlorophyceae) on acetaminophen-induced hepatotoxicity in experimental rats. *J Med Food* 7: 495-497, 2004.
55. Escapa C, Coimbra RN, Paniagua S, García AI and Otero M: Paracetamol and salicylic acid removal from contaminated water by microalgae. *J Environ Manage* 203: 799-806, 2017.
56. Hong SW, Lee HS, Jung KH, Lee H and Hong SS: Protective effect of fucoidan against acetaminophen-induced liver injury. *Arch Pharm Res* 35: 1099-1105, 2012.
57. Itoh K, Mimura J and Yamamoto M: Discovery of the negative regulator of Nrf2, Keap1: A historical overview. *Antioxid Redox Signal* 13: 1665-1678, 2010.
58. Inoue H, Maeda-Yamamoto M, Nesumi A and Murakami A: Delphinidin-3-O-galactoside protects mouse hepatocytes from (-)-epigallocatechin-3-gallate-induced cytotoxicity via up-regulation of heme oxygenase-1 and heat shock protein 70. *Nutr Res* 32: 357-364, 2012.
59. Jaiswal AK: Nrf2 signaling in coordinated activation of antioxidant gene expression. *Free Radic Biol Med* 36: 1199-1207, 2004.
60. Kensler TW, Wakabayash N and Biswal S: Cell survival responses to environmental stresses via the Keap1-Nrf2-ARE pathway. *Annu Rev Pharmacol Toxicol* 47: 89-116, 2007.
61. Jiang ZY, Xu LL, Lu MC, Chen ZY, Yuan ZW, Xu XL, Guo XK, Zhang XJ, Sun HP and You QD: Structure-activity and structure-property relationship and exploratory in vivo evaluation of the nanomolar Keap1-Nrf2 protein-protein interaction inhibitor. *J Med Chem* 58: 6410-6421, 2015.
62. Bataille AM and Manautou JE: Nrf2: A potential target for new therapeutics in liver disease. *Clin Pharmacol Ther* 92: 340-348, 2012.
63. Kong AN, Owuor E, Yu R, Hebbar V, Chen C, Hu R and Mandlekar S: Induction of xenobiotic enzymes by the MAP kinase pathway and the antioxidant or electrophile response element (ARE/EpRE). *Drug Metab Rev* 33: 255-271, 2001.
64. Nakaso K, Yano H, Fukuhara Y, Takeshima T, Wada-Isoe K and Nakashima K: PI3K is a key molecule in the Nrf2-mediated regulation of antioxidative proteins by hemin in human neuroblastoma cells. *FEBS Lett* 546: 181-184, 2003.
65. Horike N, Sakoda H, Kushiyama A, Ono H, Fujishiro M, Kamata H, Nishiyama K, Uchijima Y, Kurihara Y, Kurihara H and Asano T: AMP-activated protein kinase activation increases phosphorylation of glycogen synthase kinase 3 β and thereby reduces cAMP-responsive element transcriptional activity and phosphoenolpyruvate carboxykinase C gene expression in the liver. *J Biol Chem* 283: 33902-33910, 2008.
66. Konrad D, Rudich A, Bilan PJ, Patel N, Richardson C, Witters LA and Klip A: Troglitazone causes acute mitochondrial membrane depolarisation and an AMPK-mediated increase in glucose phosphorylation in muscle cells. *Diabetologia* 48: 954-966, 2005.
67. Luo J: The role of Glycogen synthase kinase 3 β (GSK3 β) in tumorigenesis and cancer chemotherapy. *Cancer Lett* 273: 194-200, 2009.
68. Shin SM, Cho IJ and Kim SG: Resveratrol protects mitochondria against oxidative stress through AMP-activated protein kinase-mediated glycogen synthase kinase-3 β inhibition downstream of poly(ADP-ribose)polymerase-LKBI pathway. *Mol Pharmacol* 76: 884-895, 2009.
69. Wang L, Zhang S, Cheng H, Lv H, Cheng G and Ci X: Nrf2-mediated liver protection by esculentoside A against acetaminophen toxicity through the AMPK/Akt/GSK3 β pathway. *Free Radic Biol Med* 101: 401-412, 2016.
70. Jaeschke H and Bajt ML: Intracellular signaling mechanisms of acetaminophen-induced liver cell death. *Toxicol Sci* 89: 31-41, 2006.
71. Ray SD, Mumaw VR, Raje RR and Fariss MW: Protection of acetaminophen-induced hepatocellular apoptosis and necrosis by cholesteryl hemisuccinate pretreatment. *J Pharmacol Exp Ther* 279: 1470-1483, 1996.
72. Kass GE, Macanas-Pirard P, Lee PC and Hinton RH: The role of apoptosis in acetaminophen-induced injury. *Ann NY Acad Sci* 1010: 557-559, 2003.
73. Malhi H, Gores GJ and Lemasters JJ: Apoptosis and necrosis in the liver: A tale of two deaths? *Hepatology* 43 (Suppl 1): S31-S44, 2006.
74. Bürkle A, Brabeck C, Diefenbach J and Beneke S: The emerging role of poly(ADP-ribose) polymerase-1 in longevity. *Int J Biochem Cell Biol* 37: 1043-1053, 2005.
75. Andrabi SA, Kim NS, Yu SW, Wang H, Koh DW, Sasaki M, Klaus JA, Otsuka T, Zhang Z, Koehler RC, *et al*: Poly(ADP-ribose) (PAR) polymer is a death signal. *Proc Natl Acad Sci USA* 103: 18308-18313, 2006.
76. Isabelle M, Moreel X, Gagné JP, Rouleau M, Ethier C, Gagné P, Hendzel MJ and Poirier GG: Investigation of PARP-1, PARP-2, and PARG interactomes by affinity-purification mass spectrometry. *Proteome Sci* 8: 22, 2010.
77. Alexia C, Fallot G, Lasfer M, Schweizer-Groyer G and Groyer A: An evaluation of the role of insulin-like growth factors (IGF) and of type-I IGF receptor signalling in hepatocarcinogenesis and in the resistance of hepatocarcinoma cells against drug-induced apoptosis. *Biochem Pharmacol* 68: 1003-1015, 2004.
78. Yanai R, Yamada N, Inui M and Nishida T: Correlation of proliferative and anti-apoptotic effects of HGF, insulin, IGF-1, IGF-2, and EGF in SV40-transformed human corneal epithelial cells. *Exp Eye Res* 83: 76-83, 2006.
79. Hwang HJ, Kwon MJ and Nam TJ: Chemoprotective effect of insulin-like growth factor I against acetaminophen-induced cell death in chag liver cells via ERK1/2 activation. *Toxicology* 230: 76-82, 2007.
80. Brodt P, Samani A and Navab R: Inhibition of the type I insulin-like growth factor receptor expression and signaling: Novel strategies for antimetastatic therapy. *Biochem Pharmacol* 60: 1101-1107, 2000.
81. Segrelles C, Moral M, Lara MF, Ruiz S, Santos M, Leis H, García-Escudero R, Martínez-Cruz AB, Martínez-Palacio J, Hernández P, *et al*: Molecular determinants of Akt-induced keratinocyte transformation. *Oncogene* 25: 1174-1185, 2006.
82. Lee ER, Kim JY, Kang YJ, Ahn JY, Kim JH, Kim BW, Choi HY, Jeong MY and Cho SG: Interplay between PI3K/Akt and MAPK signaling pathways in DNA-damaging drug-induced apoptosis. *Biochim Biophys Acta* 1763: 958-968, 2006.
83. Shaw RJ and Cantley LC: Ras, PI(3)K and mTOR signalling controls tumour cell growth. *Nature* 441: 424-430, 2006.
84. Bhandari BK, Feliers D, Duraisamy S, Stewart JL, Gingras AC, Abboud HE, Choudhury GG, Sonenberg N and Kasinath BS: Insulin regulation of protein translation repressor 4E-BP1, an eIF4E-binding protein, in renal epithelial cells. *Kidney Int* 59: 866-875, 2001.
85. O'Reilly KE, Rojo F, She QB, Solit D, Mills GB, Smith D, Lane H, Hofmann F, Hicklin DJ, Ludwig DL, *et al*: mTOR inhibition induces upstream receptor tyrosine kinase signaling and activates Akt. *Cancer Res* 66: 1500-1508, 2006.
86. Treisman R: Regulation of transcription by MAP kinase cascades. *Curr Opin Cell Biol* 8: 205-215, 1996.
87. Gunawan BK, Liu ZX, Han D, Hanawa N, Gaarde WA and Kaplowitz N: c-Jun N-terminal kinase plays a major role in murine acetaminophen hepatotoxicity. *Gastroenterology* 131: 165-178, 2006.
88. Wang KP, Bai Y, Wang J and Zhang JZ: Inhibitory effects of *Schisandra chinensis* on acetaminophen-induced hepatotoxicity. *Mol Med Rep* 9: 1813-1819, 2014.
89. Dews M, Prisco M, Peruzzi F, Romano G, Morrione A and Baserga R: Domains of the insulin-like growth factor I receptor required for the activation of extracellular signal-regulated kinases. *Endocrinology* 141: 1289-1300, 2000.
90. Prasad R, Vaid M and Katiyar SK: Grape proanthocyanidin inhibit pancreatic cancer cell growth in vitro and in vivo through induction of apoptosis and by targeting the PI3K/Akt pathway. *PLoS One* 7: e43064, 2012.

